Journal of Magnetic Resonance 307 (2019) 106577

Contents lists available at ScienceDirect

Journal of Magnetic Resonance

journal homepage: www.elsevier.com/locate/jmr

Decoupled LIGHT-SABRE variants allow hyperpolarization of asymmetric SABRE systems at an arbitrary field

Jacob R. Lindale [a], Christian P.N. Tanner [a], Shannon L. Eriksson [a,b], Warren S. Warren [c,*]

[a] Department of Chemistry, Duke University, Durham, NC 27708, United States
[b] School of Medicine, Duke University, Durham, NC 27708, United States
[c] Departments of Physics, Chemistry, Biomedical Engineering, and Radiology, Duke University, Durham, NC 27708, United States

ARTICLE INFO

Article history:
Received 10 March 2019
Revised 14 August 2019
Accepted 16 August 2019
Available online 17 August 2019

Keywords:
Hyperpolarization
SABRE
Co-ligands
High field
Pulse sequences

ABSTRACT

Signal Amplification By Reversible Exchange, or SABRE, uses the singlet-order of parahydrogen to generate hyperpolarized signals on target nuclei, bypassing the limitations of traditional magnetic resonance. Experiments performed directly in the magnet provide a route to generate large magnetizations continuously without having to field-cycle the sample. For heteronuclear SABRE, these high-field methods have been restricted to the few SABRE complexes that exhibit efficient exchange with symmetric ligand environments as co-ligands induce chemical shift differences between the parahydrogen-derived hydrides, destroying the hyperpolarized spin order. Through careful consideration of the underlying spin physics, we introduce ^{1}H decoupled LIGHT-SABRE pulse sequence variants which bypasses this limitation, drastically expanding the scope of heteronuclear SABRE at high field.

Hyperpolarization methods overcome the intrinsic insensitivity of magnetic resonance methods by artificially inducing polarizations much larger than those obtained under thermal conditions [1–4]. Brute force hyperpolarization is possible by cooling, but for ^{1}H at 10 Tesla, the energy difference between spin states in temperature units (E/k_B) is 20 mK, and at such temperatures T_1 is very long, so the growth of magnetization is very slow for almost all molecules [5,6]. Thus, the most commonly used methods derive nuclear spin order from another source, including electron spin order (DNP) [1,7–11], light-induced radical pair generation (CIDNP) [2,12–14], and light angular momentum pumping (SEOP) [15–18]. A particularly interesting source of spin order is found in parahydrogen (p-H_2), the $2^{-½}(\alpha\beta-\beta\alpha)$ spin isomer of the hydrogen molecule, as it is readily prepared under mild conditions (such as cooling to 77 K in the presence of an iron oxide catalyst) and can be generated in large quantities. Parahydrogen was first demonstrated as a hyperpolarization source in the original Parahydrogen Induced Polarization (PHIP) [3,4] experiments, where p-H_2 was catalytically added across a bond. Signal Amplification By Reversible Exchange (SABRE) [19–21] is a more recent, non-reactive variant of PHIP, which utilizes transient binding of target ligands and parahydrogen to an iridium "polarization transfer catalyst" (PTC) to unlock the p-H_2 singlet order. While the original SABRE experiment generates hyperpolarized ^{1}H magnetization, more recent variants [22–26], which we collectively call heteronuclear or X-SABRE, have several significant advantages over other hyperpolarization approaches. These experiments can produce >25% spin polarization on heteronuclei in under a minute at room temperature [27] on hundreds of different molecules to date [28–31], and have the added benefit that heteronuclear T_1 relaxation is often significantly slower than it is for protons, given the smaller magnitude of the dipolar couplings. Furthermore, X-SABRE methods show great promise as a new method in providing continuous hyperpolarization to biomedical imaging contrast agents [32,33].

Broadly, SABRE hyperpolarization is generated by allowing population to flow out of the initial singlet state into target states by inducing level anti-crossings (LACs) that allow these states to mix. In the original SABRE work [19], such LACs are facilitated by a static magnetic field at a strength where the resonance frequency difference between the bound parahydrogen (hydride) protons and the target's protons was comparable to the hydride J-coupling (about 6 mT); J-couplings between the hydride protons and the target's protons can then create observable magnetization on the target. For direct polarization of heteroatoms (most commonly ^{15}N), such as in the SABRE-SHEATH [22] experiment, these anti-crossings take place at still lower fields of ~0.5 μT, or 1% of the Earth's field. Such conditions are easily accessible in the lab with a μ-metal shield and a small coil. Traditional SABRE experiments utilize a steady-state scheme to generate hyperpolarization on target ligands, continuously or quasi-continuously exposing the

* Corresponding author.
E-mail address: warren.warren@duke.edu (W.S. Warren).

https://doi.org/10.1016/j.jmr.2019.106577
1090-7807/

sample to the LAC condition for much longer (~10–90 s) than the lifetime of the hyperpolarization active species (~20–50 ms). More recently, it has been shown that coherently pumping the system with pulse-lengths on the order of the lifetime of the system can significantly enhance polarization transfer in both the high-field and low-field regimes, and introduced a quantum Monte Carlo (QMC) based simulation method to describe the resulting complex dynamics [34].

An alternative strategy which works at an arbitrarily high field uses a slightly different avoided curve crossing to create large heteronuclear magnetization just by adding micro-watts of resonant radio-frequency irradiation. This was realized in the LIGHT-SABRE [24] and RF-SABRE [25,35] experiments, which directly access the singlet spin order to generate hyperpolarization using a Spin Lock Induced Crossing (SLIC) pulse. While the original LIGHT-SABRE pulse sequence utilizes on-resonance excitation to pump x-magnetization that is then stored along B_z with a selective pulse, newer variants [34,36,37] utilize off-resonance excitation to directly pump z-magnetization, significantly boosting signal enhancements. Similarly, coherence transfer methods may be utilized at high field to generate heteronuclear polarization with INEPT or ADAPT pulse sequence variants [20,38,39].

The high field methods have some obvious advantages (for example, they can be done directly in the imaging magnet) but have generally not been as efficient as the low field methods. An important reason has to do with the symmetry of the hydride complex. The most common catalysts bind two ligands symmetrically, keeping the two *p*-H_2 derived hydride atoms chemically equivalent and preserving the singlet long enough for transfer to occur. However, many substrates additionally require a co-ligand such as pyridine to activate the complex, and others bind only a single ligand [28,40]. Thus, it is very common for the two hydride atoms to be inequivalent. In this case the chemical shift difference (often on the order of several hundred Hertz at high field) causes rapid interconversion between $S_H = (\alpha\beta - \beta\alpha)/\sqrt{2}$ and one of the triplet states, $T_H^0 = (\alpha\beta + \beta\alpha)/\sqrt{2}$. In fact, the cleanest demonstrations of LIGHT-SABRE and related approaches have been on systems such as pyridine itself, where this asymmetry disappears. This has seriously restricted the applicability of the SLIC-based high field methods. Here we carefully examine the spin physics to show that small modifications to the LIGHT-SABRE pulse sequence, such as incorporating simple CW-decoupling and introducing a targeted recoupling between singlet and triplet states, significantly extends the scope and efficiency of heteronuclear high field SABRE experiments to include systems with asymmetric ligand environments.

As a concrete example, we focus here on mixtures of ^{15}N-acetonitrile (ACN) and pyridine (pyr) at natural abundance. This together forms an ABX spin system (Fig. 1) with chemically inequivalent hydrides ($\hat{I}$ and $\hat{I}'$) and a single ^{15}N-nucleus ($\hat{S}$), and is a good chemical model to utilize for the applications explored here. The Hamiltonian in a doubly rotating frame, which for spins $\hat{I}$and $\hat{I}'$ is rotated about the center of the hydride resonances and rotating around the center frequency of the $\hat{S}$ spin, has the form:

$$\hat{H} = \frac{\Delta\omega_{HH}}{2}\left(\hat{I}_z - \hat{I}'_z\right) + \Delta\omega_N\hat{S}_z + \omega_{1,N}\hat{S}_x + J_{HH'}\left(\hat{I}\cdot\hat{I}'\right) + J_{NH}\hat{I}_z\hat{S}_z + J_{NH'}\hat{I}'_z\hat{S}_z \quad (1)$$

$\Delta\omega_N$ is the resonance offset of the SLIC pulse from the nitrogen resonance, $\omega_{1,N}$ is the nutation frequency of the pulse,$\Delta\omega_{HH}$ is the hydride-hydride chemical shift difference, and $\Delta J_{NH} \equiv J_{NH} - J_{NH'}$. The eight energy levels will be written in the singlet-triplet basis for the hydrides $\left(T_H^{+1}, T_H^0, T_H^{-1}, S_H\right)$ and the α_N, β_N basis for the nitrogen. In the idealized case, the initial population will be enriched in singlet by an amount which depends on the temperature of preparation of the parahydrogen, and will have some fractional and evenly-distributed population between the triplet states. Population in the energy levels $T_H^{\pm1}$ (which in product operator form have the spin order $\pm\left(\frac{1}{4}\hat{E} + \hat{I}_z\hat{I}'_z\right) + \hat{I}_z + \hat{I}'_z$($\hat{E}$ is the identity operator)) commutes with the Hamiltonian in Eq. (1), so the Liouville-van Neumann equation $\dot{\rho} = i\hbar^{-1}\left[\rho, \hat{H}\right]$ implies that such population never evolves into spin order $\hat{S}_z$. The remaining hyperpolarization-active subspace of the Hamiltonian for this system is given by:

$$\hat{H} = \begin{array}{c} \\ T_H^0\alpha_N \\ T_H^0\beta_N \\ S_H\alpha_N \\ S_H\beta_N \end{array} \begin{array}{c} \begin{array}{cccc} T_H^0\alpha_N & T_H^0\beta_N & S_H\alpha_N & S_H\beta_N \end{array} \\ \begin{pmatrix} \Delta\omega_N + 2\pi J_{HH} & \omega_{1,N} & \frac{1}{2}(\Delta\omega_{HH} + \pi\Delta J_{NH}) & 0 \\ \omega_{1,N} & 2\pi J_{HH} & 0 & \frac{1}{2}(\Delta\omega_{HH} - \pi\Delta J_{NH}) \\ \frac{1}{2}(\Delta\omega_{HH} + \pi\Delta J_{NH}) & 0 & \Delta\omega_N & \omega_{1,N} \\ 0 & \frac{1}{2}(\Delta\omega_{HH} - \pi\Delta J_{NH}) & \omega_{1,N} & 0 \end{pmatrix} \end{array} \quad (2)$$

For the hydride spin pair, the S_H and T_H^0 states interconvert at a rate proportional to the hydride-hydride chemical shift difference, $\Delta\omega_{HH}$. If this is rapid compared to the other terms (which will typically be the case at 1 Tesla or above), and particularly in a system where exchange is rapid, it is simplest to view the chemical shift difference as equilibrating the populations of the S_H and T_H^0 states; and such an initial state $\left(S_H + T_H^0 = \frac{1}{2}\hat{E} - \hat{I}_z\hat{I}'_z\right)$ *also* commutes with the Hamiltonian, similar to the PASADENA conditions [41]. Thus, the interesting dynamics comes only from the "flip-flop" portion of the singlet state operator $S_H - \hat{I}_z\hat{I}'_z = \frac{1}{4}\hat{E} - \hat{I}\cdot\hat{I}' = \hat{I}_x\hat{I}'_x + \hat{I}_y\hat{I}'_y$; in other words, there must be a population difference between S_H and T_H^0.

To gain an understanding of the underlying spin operator pathways that lead to the generation of hyperpolarized S_z spin order, we evaluate the Taylor series expansion of the evolving density matrix as:

$$\begin{aligned}\hat{\rho}(t) &\approx \sum_{n=0}^{\infty}\frac{\partial_t^n\hat{\rho}}{n!}t^n \\ &= \hat{\rho}_0 + \frac{i^1}{1!}\left[\hat{\rho}, \hat{H}\right]t^1 + \frac{i^2}{2!}\left[\left[\hat{\rho}, \hat{H}\right], \hat{H}\right]t^2 \\ &\quad + \frac{i^3}{3!}\left[\left[\left[\hat{\rho}, \hat{H}\right], \hat{H}\right], \hat{H}\right]t^3 + \cdots\end{aligned} \quad (3)$$

Since we are interested in producing $\hat{S}_z$, we can start from $\hat{I}_x\hat{I}'_x + \hat{I}_y\hat{I}'_y$ as discussed above. If we ignore chemical shift difference between the hydride protons, there are a divergent number of

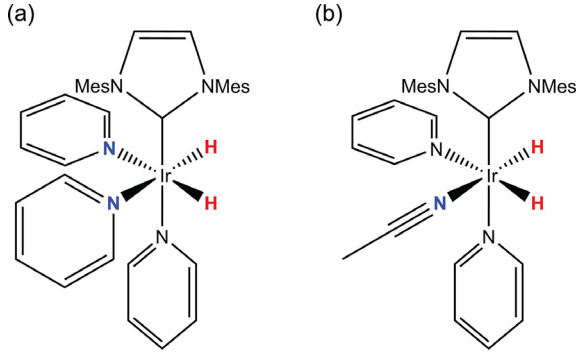

Fig. 1. Model SABRE systems. (a) The 4-spin AA′XX′ $[Ir(H)_2(IMes)(^{15}N\text{-}pyr)_3]^+$ canonical SABRE system. (b) The 3-spin ABX $[Ir(H)_2(IMes)(pyr)_2(^{15}N\text{-}ACN)]^+$ SABRE system. Colored atoms indicate spin-1/2 nuclei that form the SABRE system.

pathways that lead eventually to $\widehat{S}_z$ order. The leading term in the expansion affords the most direct spin operator pathway to generate hyperpolarized $\widehat{S}_z$ magnetization, and is given by:

$$\widehat{S}_z(t) \propto \Delta J_{NH}\omega_{1,N}J_{HH}\Delta J_{NH}\Delta\omega_N\omega_{1,N}t^6 \quad (4)$$

Eq. (4) is written in the order of commutation required to generate $\widehat{S}_z$; for instance, the first derivative is given by the commutator $i\left[\widehat{I}_x\widehat{I}'_x+\widehat{I}_y\widehat{I}'_y,\Delta J_{NH}\widehat{I}_z\widehat{S}_z\right]=\Delta J_{NH}\left(\widehat{I}_y\widehat{I}'_x-\widehat{I}_x\widehat{I}'_y\right)\widehat{S}_z$ and so on (see SI for details). The power dependence given in Eq. (4) indicates that the ΔJ_{NH} coupling must act twice: once to generate coherences between the hydrides and nitrogen spin, and a second time in conjunction with the "flip-flop" term $\widehat{I}_x\widehat{I}'_x+\widehat{I}_y\widehat{I}'_y$ in J_{HH} to reduce these same coherences to single spin order on the nitrogen. Introducing a chemical shift difference truncates the hydride interaction to the first order term $\widehat{I}_z\widehat{I}'_z$, eliminating this pathway. Also, while changing the sign of the resonance offset changes the sign of the magnetization, the squared dependence on $\omega_{1,N}$ indicates that changing the phase of the pulse does not change the sign of $\widehat{S}_z$, as to be expected given that the pulse phase is arbitrary in space. Of course, exact (numerical) calculations are also possible (See SI for details), but this expansion gives insight. For example, as we show in the SI, both the original form of LIGHT-SABRE and SABRE-SHEATH have leading terms which scale as t^4, and this is an important difference particularly for rapidly exchanging ligands. Remarkably, the exact calculations of the dynamics approximately rise on the order of time predicted by the leading terms in the expansion for all three conditions for the first 10 ms in the dynamics (Fig. 2).

In order to preserve the full form of the singlet order and the strong coupling limit of the J_{HH} coupling, we use CW decoupling with a ^{1}H irradiation power exceeding the chemical shift difference of the hydrides and with a carrier frequency at the center of the two resonances. Essentially, the CW decoupling can be thought of as a spin-lock in a tilted frame [42] to maintain the singlet character of the parahydrogen-derived hydrides, similar to previous high field methods for maintaining singlet states [43], and to retain the strong coupling limit of the hydride-hydride coupling. During the inter-pulse delays, we utilize broadband decoupling to continue to efficiently continue decoupling, but are not constrained in the same way to preserve the tilted frame. In the absence of this decoupling, the S_H and T^0_H populations pump oppositely signed magnetization in the case of both equivalent and inequivalent hydrides (Fig. 3a). ^{1}H decoupling allows the hyperpolarization dynamics to evolve in the case of asymmetric systems (Fig. 3b), which starts from a 100% hyperpolarized singlet state in the simulation.

While simultaneous ^{1}H/^{15}N irradiation has been considered for previous high-field pulse sequences to generate a LAC in a doubly rotating frame [44], our approach is fundamentally different as the

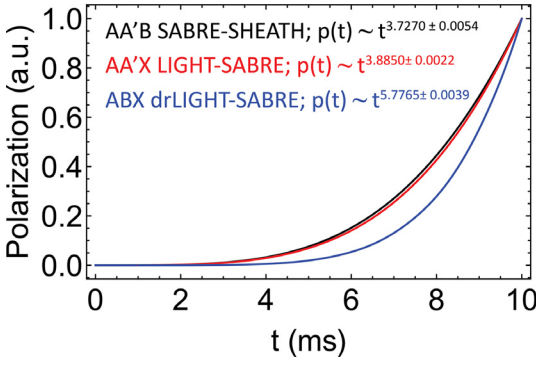

Fig. 2. Initial trajectory of evolution for SABRE-SHEATH, on-resonance LIGHT-SABRE, and off-resonance decoupled LIGHT-SABRE sequences used here. All three cases rise approximately as the order of time predicted by the Talyor expansion, with SABRE-SHEATH and LIGHT-SABRE rising as ~t^4 and drLIGHT-SABRE rising as t^6.

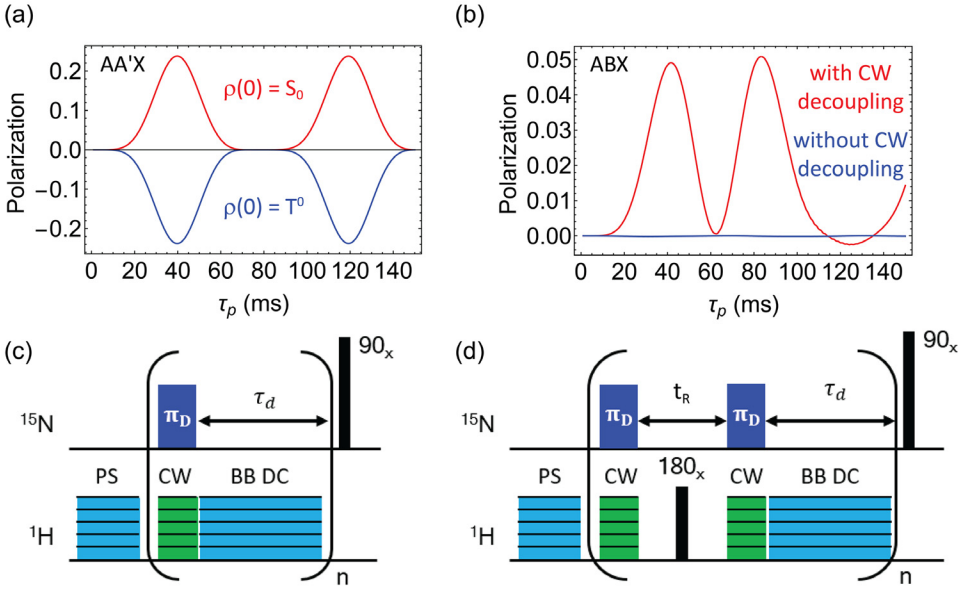

Fig. 3. Basic of decoupling schemes for LIGHT-SABRE experiments of asymmetric complexes. (a) The hydride S_H and T^0_H populations pump opposite-sign magnetization in high field experiments with chemically equivalent hydrides (AA'X system) using only a SLIC-pulse of length τ_p. (b) In asymmetric ligand environements, the equilibration between singlet and triplet-0 populations prevents polarization. Adding CW decoupling pulses tuned to the center of the hydride resonances recovers hyperpolarization. (c) The decoupled LIGHT-SABRE (dLIGHT) and (d) the decoupled-recoupled LIGHT-SABRE (drLIGHT) pulse sequences are two different methods built on the basis of the simulations shown in (b), both using variable power decoupling to suppress S_H-T^0_H equilibration. To maximize polarization, the pulse is applied for a time long enough to achieve a p-pulse in the hyperpolarization dynamics (π_D), maximizing the signal. In the drLIGHT experiment, a recoupling time t_R is introduced to interchange the S_H-T^0_H populations after the SLIC-pulse. Both experiments use either CW or broadband (PS/BB) decoupling, with the only distinction between the latter is that PS is applied for 4 s and BB DC is applied for the inter-pulse delay τ_d. All decoupling pulses are given with equivalent powers.

LAC condition itself ($\omega_{1,H} \approx \Delta\omega_{HH}$) is not used; rather, we use a higher field to decouple the singlet evolution. We also note that a modified SLIC-SABRE method has recently been introduced to extract hyperpolarization from anti-phase spin order by conversion of $\widehat{I}_z\widehat{I}'_z \rightarrow \widehat{I}_x\widehat{I}'_x$ using a 90_y pulse, but this only works with chemically equivalent hydrides [36,45] as $\widehat{I}_x\widehat{I}'_x$ order rapidly dephases in the absence of a spin-lock, so this would result in no generation of hyperpolarized $\widehat{S}_z$ spin order.

The decoupled LIGHT-SABRE (dLIGHT) experiment (Fig. 3c) adds various decoupling pulses to the ^{1}H channel and, similar to newer iterations of SLIC-based pulse sequences, utilizes off-resonance excitation to directly generate z-magnetization, thus negating the need for a storage pulse as in the original LIGHT-SABRE experiment. Furthermore, this pulse sequence is constructed as a coherently pulsed experiment, where short delays (~100 ms) interrupt the coherent evolution to allow for chemical exchange. Doing so significantly enhances the control over the spin dynamics, allowing for a targeted improvement of the pulse sequence performance. Fig. 3d shows a different variant, the drLIGHT experiment; as each SLIC pulse generates some T_H^0 population, we may take advantage of the ability to interchange S_H and T_H^0 populations given by equation by recoupling the hydrides (removing the decoupling pulses) for a short period of time. Immediately thereafter, the system is poised to be pumped again with a secondary ^{1}H-decoupled SLIC pulse.

Experiments were performed in a Bruker 360DX spectrometer using a sample comprised of 75 mM ^{15}N-acetonitrile and 33 mM pyridine, at natural abundance with 5 mM [Ir(IMes)(COD)]Cl (IMes = 1,3-bis(2,4,6-trimethylphenyl)imidazol-2-ylidene, COD = 1,5-cyclooctadiene) pre-catalyst dissolved in methanol d_4. Parahydrogen at a 50% enrichment was generated by flowing hydrogen gas over iron (III) oxide at 77 K and continuously flowed through the system with a 5 mm medium-walled NMR tube. The sample was allowed to activate for 25 min at room temperature prior to running any of the experiments. The bubbling flow rate is limited by the ability to lock on the sample, and was approximately 40 sccm/min with a head pressure of ~8.3 bar. Importantly, the parahydrogen flow is turned off 3 s prior to acquisition to remove the inhomogeneities introduced by the bubbling. The pre-saturation and inter-pulse decoupling conditions utilize the same power as the CW pulse with a broadband composite pulse decoupling, but are applied for 4 s in the case of the pre-saturation segment and for the entire length of the inter-pulse delay for the broadband decoupling (BB DC). All experiments utilize a coherent SLIC-pulse with $\omega_{1,N}$ =11 Hz and $\Delta\omega_N = -20$ Hz; the optimization of other pulse sequence parameters, such as the pulse length τ_p was done experimentally. The optimal pulse length will generate a π-pulse in the hyperpolarization dynamics (π_D), inverting the populations between the initial singlet and target states [40].

The efficacy of the decoupled LIGHT-SABRE pulse sequences is demonstrated in Fig. 4. The decoupling frequency is tuned to the center of the two hydride resonances (Fig. 4a), where the downfield resonance corresponds to the hydride trans to the ^{15}N-ACN, as indicated by the additional 24 Hz splitting indicative of the $^2J_{NH}$ coupling. Fig. 4b shows that the S_H order is efficiently preserved when the CW power exceeds the chemical shift difference, indicated by the line in red. Then, using $\omega_{1,H}$ =1600 Hz for the decoupling sequences with an optimal π-pulse at τ_p = 24 ms, one can obtain an enhancement of $\varepsilon = 57.6$ from the dLIGHT pulse sequence. For these experiments, the optimal inter-pulse delay is found to be 25 ms, just as shown previously on symmetric systems. The enhancement from an inter-pulse delay of 100 ms was $\varepsilon = 20.4$, which indicates that perhaps the sample is being moved out of the active region of the coil by the bubbling, allowing for larger polarizations with smaller delays.

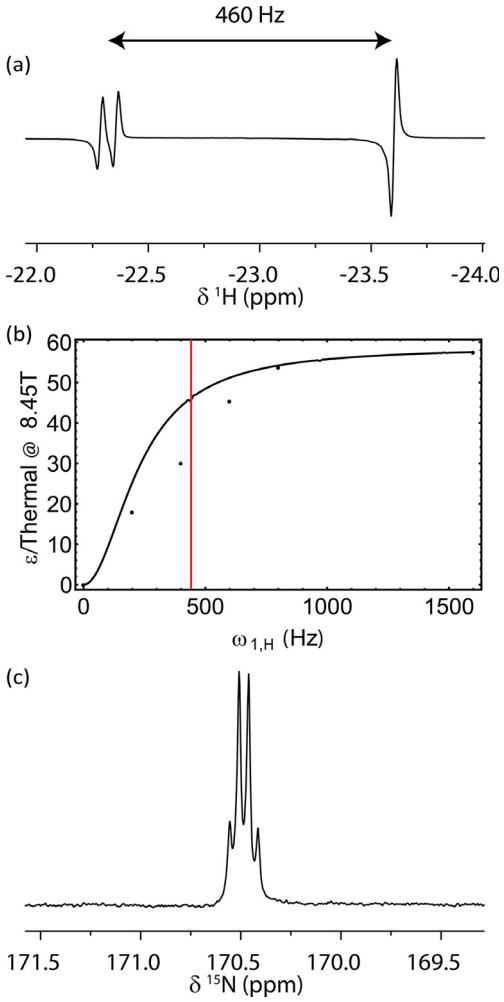

Fig. 4. Decoupled LIGHT-SABRE allows hyperpolarization of asymmetric complexes at an arbitrary field, shown here using [Ir(H)$_2$(IMes)(pyr)$_2$(^{15}N-ACN)]$^+$. (a) The parahydrogen-derived hydride spectrum, where the upfield proton is trans to the ^{15}N-acetonitrile. (b) Power dependence of dLIGHT signal shown with theory result (black) and with $\Delta\omega_{HH}$ (red). (c) dr-LIGHT spectrum of ^{15}N-acetonitrile, using a B_1 power of 1600 Hz for both the CW and BB decoupling, yielding an enhancement of 101-fold over thermal ^{15}N polarization after optimization of the bubbling. (For interpretation of the references to colour in this figure legend, the reader is referred to the web version of this article.)

For the drLIGHT-SABRE pulse sequence, the π_D-pulse length was found to be 18 ms with an optimized refocusing time of t_R = 250 μs. Note that this is only about 25% of the time needed to completely interchange the population between S_H and T_H^0 (=1/2 * (460 Hz) = 1090 μs) Since, ignoring any coherences, the observable nitrogen signal is proportional to the difference in population between S_H and T_H^0 states (as discussed earlier), it is not possible to "deplete" the singlet state and then "add population back in" from the triplet successfully; the best that can be done is to equilibrate the populations. However, for the ligands which have not exchanged, creation of nitrogen polarization also implies creating a coherence between S_H and T_H^0, and that can be returned to larger S_H population by the resonance offset. In practice, the delay boosts polarization and a maximum enhancement of $\varepsilon = 101$ is obtained. This polarization is achieved with inter-pulse delays of 100 ms and when the π_x pulse is used between the two drLIGHT pulses to invert the T_H^+ and T_H^- populations. Omitting the π_x for the same conditions gives an enhancement of $\varepsilon = 53.7$. Interestingly, the same pulse sequence with a delay-length of 25 ms gave an enhancement of only $\varepsilon = 3.4$, which is in stark contrast

to the dLIGHT variant. This may arise due to the fact in the regime where the delay-length is short, that multiple loops begins to pump opposite-sign magnetization.

We have furthered the uses of the drLIGHT sequence by examining the ^{15}N-^{13}C-acetonitirile system, which generates hyperpolarized magnetization by pumping off resonance of the bound nitrogen spin (Fig. 5) with an enhancement of $\varepsilon = 146$ or can generate hyperpolarized heteronuclear anti-phase spin order like $\widehat{I}_{z,N}\widehat{S}_{z,C}$ by pumping on resonance of the bound nitrogen spin, which yielded an enhancement of $\varepsilon = 97$. The spin lattice relaxation of the $\widehat{I}_{z,N}$ spin order was measured to be $T_1 = 72.4 \pm 2.4\ s$ at this field, whereas the relaxation of the anti-phase spin order was measured to be $T_1 = 22.0 \pm 1.5\ s$, as to first order the relaxation of $\widehat{I}_{z,N}\widehat{S}_{z,C}$ should relax as $\frac{1}{T_{1,C}} + \frac{1}{T_{1,N}}$.

In regards to the limitations of the decoupled LIGHT-SABRE pulse sequences, theoretical explorations with the QMC simulation method of additional regions of parameter space and subsequent experimental optimization of these systems may provide enhanced performance of these sequences. Previously, we have shown that the use of shaped pulses, including both linear and non-linear ramps [34,46], provides significantly better polarization than using square-pulses. Furthermore, optimizing the consumption of singlet order with multi-pulse schemes, like the drLIGHT sequence introduced here, may further push the polarizations obtained by these sequences on asymmetric systems.

The methods introduced here are a simple path to accessing a significantly broader scope of SABRE targets at high field. Obvious extensions, such as proton pulse sequences which remove the population from T_H^0, will likely provide further improvements. The decoupled LIGHT-SABRE method also allows use of phosphinooxazoline-based SABRE catalysts [40] at high field, which allow hyperpolarization of sterically-hindered substrates but always induce a chemical shift difference between the hydrides. Increasing the scope of SABRE also allows exploration of the possibility of accessing relaxation-protected eigenstates at high field, providing a possible new method to generate long-lived molecular imaging tags directly in the magnet.

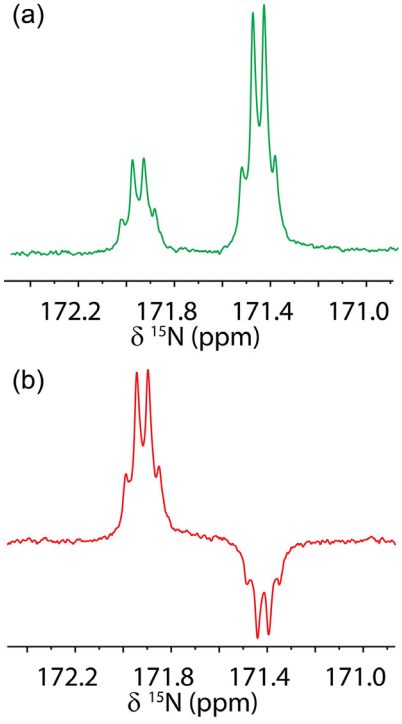

Fig. 5. drLIGHT spectra of asymmetric spin systems generated by [Ir(H)$_2$(IMes)(pyr)$_2$(^{15}N-^{13}C-ACN)]$^+$ SABRE complexes at 8.45 T. (a) Hyperpolarized magnetization on ^{15}N-^{13}C-acetonitrile with with ε = 146. (b) Hyperpolarized heteronuclear anti-phase spin order between ^{15}N-^{13}C spins with ε = 97, with a relaxation time is T_1 = 22 ± 1.5 s at this field.

Acknowledgements

The authors thank the following funding source: NSF CHE-1665090. Research reported in this publication was also supported by the National Institute of Biomedical Imaging and Bioengineering of the NIH under R21EB025313 and R21EB026153. J. R. L. thanks Nathan J. Adamson (Duke University, Department of Chemistry) and Dr. Steven J. Malcolmson for the synthesis of the [Ir(IMes)(COD)]Cl pre-catalyst.

Declaration of Competing Interest

The authors declare no conflict of interest.

Appendix A. Supplementary material

Supplementary data to this article can be found online at https://doi.org/10.1016/j.jmr.2019.106577.

References

[1] J.H. Ardenkjaer-Larsen, B. Fridlund, A. Gram, G. Hansson, L. Hansson, M.H. Lerche, R. Servin, M. Thaning, K. Golman, Increase in signal-to-noise ratio of >10,000 times in liquid-state NMR, Proc. Natl. Acad. Sci. U.S.A. 100 (2003) 10158–10163.
[2] G. Vermeersch, J. Marko, N. Febvaygarot, S. Caplain, A. Lablachecombier, Low-field photochemically induced dynamic nuclear-polarization (photo-CIDNP) of diazanaphthalenes, J. Chem. Soc.-Perkin Trans. 2 (1984) 2027–2030.
[3] C.R. Bowers, D.P. Weitekamp, Transformation of symmetrization order to nuclear-spin magnetization by chemical-reaction and nuclear-magnetic-resonance, Phys. Rev. Lett. 57 (1986) 2645–2648.
[4] C.R. Bowers, D.P. Weitekamp, Para-hydrogen and synthesis allow dramatically enhanced nuclear alignment, J. Am. Chem. Soc. 109 (1987) 5541–5542.
[5] M.L. Hirsch, B.A. Smith, M. Mattingly, A.G. Goloshevsky, M. Rosay, J.G. Kempf, Transport and imaging of brute-force 13C hyperpolarization, J. Magn. Reson. 261 (2015) 87–94.
[6] J.S. Waugh, P.C. Hammel, P.L. Kuhns, O. Gonen, Spin-lattice relaxation below 1K, Bull. Mag. Res. 11 (1989) 97–102.
[7] A. Abragam, M. Goldman, Principles of dynamic nuclear polarisation, Rep. Prog. Phys. 41 (1978) 395.
[8] A.B. Barnes, G. De Paëpe, P.C.A. van der Wel, K.N. Hu, C.G. Joo, V.S. Bajaj, M.L. Mak-Jurkauskas, J.R. Sirigiri, J. Herzfeld, R.J. Temkin, R.G. Griffin, High-field dynamic nuclear polarization for solid and solution biological NMR, Appl. Magn. Reson. 34 (2008) 237–263.
[9] A. Bornet, R. Melzi, A.J.P. Linde, P. Hautle, B. van den Brandt, S. Jannin, G. Bodenhausen, Boosting dissolution dynamic nuclear polarization by cross polarization, J. Phys. Chem. Lett. 4 (2013) 111–114.
[10] S. Jannin, A. Bornet, S. Colombo, G. Bodenhausen, Low-temperature cross polarization in view of enhancing dissolution dynamic nuclear polarization in NMR, Chem. Phys. Lett. 517 (2011) 234–236.
[11] T.F. Prisner, Dynamic Nuclear Polarization, NMR of Biomolecules, Wiley-VCH Verlag GmbH & Co. KGaA, 2012, pp. 419–431.
[12] M. Goez, Photo-CIDNP spectroscopy, Annu. Rep. NMR Spectrosc. 66 (66) (2009) 77–147.
[13] M. Goez, Elucidating organic reaction mechanisms using Photo-CIDNP spectroscopy, Hyperpolariz. Methods NMR Spectrosc. 338 (2013) 1–32.
[14] K.L. Ivanov, K. Miesel, A.V. Yurkovskaya, S.E. Korchak, A.S. Kiryutin, H.M. Vieth, Transfer of CIDNP among coupled spins at low magnetic field, Appl. Magn. Reson. 30 (2006) 513–534.
[15] T.G. Walker, W. Happer, Spin-exchange optical pumping of noble-gas nuclei, Rev. Mod. Phys. 69 (1997) 629–642.
[16] S. Appelt, A.B. Baranga, C.J. Erickson, M.V. Romalis, A.R. Young, W. Happer, Theory of spin-exchange optical pumping of He-3 and Xe-129, Phys. Rev. A 58 (1998) 1412–1439.
[17] P. Nikolaou, A.M. Coffey, M.J. Barlow, M. Rosen, B.M. Goodson, E.Y. Chekmenev, Temperature-ramped 129Xe spin exchange optical pumping, Anal. Chem. 86 (2014) 8206–8212.
[18] W.C. Chen, T.R. Gentile, Q. Ye, T.G. Walker, E. Babcock, On the limits of spin-exchange optical pumping of 3He, J. Appl. Phys. 116 (2014) 014903.

[19] R.W. Adams, J.A. Aguilar, K.D. Atkinson, M.J. Cowley, P.I. Elliott, S.B. Duckett, G. G. Green, I.G. Khazal, J. Lopez-Serrano, D.C. Williamson, Reversible interactions with para-hydrogen enhance NMR sensitivity by polarization transfer, Science 323 (2009) 1708–1711.
[20] K.D. Atkinson, M.J. Cowley, S.B. Duckett, P.I.P. Elliott, G.G.R. Green, J. Lopez-Serrano, I.G. Khazal, A.C. Whitwood, Para-hydrogen induced polarization without incorporation of para-hydrogen into the analyte, Inorg. Chem. 48 (2009) 663–670.
[21] K.D. Atkinson, M.J. Cowley, P.I.P. Elliott, S.B. Duckett, G.G.R. Green, J. Lopez-Serrano, A.C. Whitwood, Spontaneous transfer of parahydrogen derived spin order to pyridine at low magnetic field, J. Am. Chem. Soc. 131 (2009) 13362–13368.
[22] T. Theis, M.L. Truong, A.M. Coffey, R.V. Shchepin, K.W. Waddell, F. Shi, B.M. Goodson, W.S. Warren, E.Y. Chekmenev, Microtesla SABRE enables 10% nitrogen-15 nuclear spin polarization, J. Am. Chem. Soc. 137 (2015) 1404–1407.
[23] Z. Zhou, J. Yu, J.F. Colell, R. Laasner, A. Logan, D.A. Barskiy, R.V. Shchepin, E.Y. Chekmenev, V. Blum, W.S. Warren, Long-lived 13C2 nuclear spin states hyperpolarized by parahydrogen in reversible exchange at microtesla fields, J. Phys. Chem. Lett. 8 (2017) 3008–3014.
[24] T. Theis, M. Truong, A.M. Coffey, E.Y. Chekmenev, W.S. Warren, LIGHT-SABRE enables efficient in-magnet catalytic hyperpolarization, J. Magn. Reson. 248 (2014) 23–26.
[25] A.N. Pravdivtsev, A.V. Yurkovskaya, H.-M. Vieth, K.L. Ivanov, RF-SABRE: a way to continuous spin hyperpolarization at high magnetic fields, J. Phys. Chem. B 119 (2015) 13619–13629.
[26] A.N. Pravdivtsev, A.V. Yurkovskaya, H.-M. Vieth, K.L. Ivanov, Spin mixing at level anti-crossings in the rotating frame makes high-field SABRE feasible, Phys. Chem. Chem. Phys. (2014), https://doi.org/10.1039/C1034CP03765K.
[27] D.A. Barskiy, R.V. Shchepin, A.M. Coffey, T. Theis, W.S. Warren, B.M. Goodson, E. Y. Chekmenev, Over 20%15N hyperpolarization in under one minute for metronidazole, an antibiotic and hypoxia probe, J. Am. Chem. Soc. 138 (2016) 8080–8083.
[28] J.F.P. Colell, A.W.J. Logan, Z. Zhou, R.V. Shchepin, D.A. Barskiy, G.X. Ortiz, Q. Wang, S.J. Malcolmson, E.Y. Chekmenev, W.S. Warren, T. Theis, Generalizing, extending, and maximizing nitrogen-15 hyperpolarization induced by parahydrogen in reversible exchange, J. Phys. Chem. Phys. C (2017), Cover Article just accepted.
[29] Q. Wang, K. Shen, A.W.J. Logan, J.F.P. Colell, J. Bae, G.X. Ortiz Jr., T. Theis, W.S. Warren, S.J. Malcolmson, Diazirines as potential molecular imaging tags: probing the requirements for efficient and long-lived SABRE-induced hyperpolarization, Angew. Chem. Int. Ed. (2017).
[30] T. Theis, G.X. Ortiz Jr., A.W. Logan, K.E. Claytor, Y. Feng, W.P. Huhn, V. Blum, S.J. Malcolmson, E.Y. Chekmenev, Q. Wang, W.S. Warren, Direct and cost-efficient hyperpolarization of long-lived nuclear spin states on universal (15)N2-diazirine molecular tags, Sci. Adv. 2 (2016) e1501438.
[31] K. Shen, A.W. Logan, J.F. Colell, J. Bae, G.X. Ortiz Jr, T. Theis, W.S. Warren, S.J. Malcolmson, Q. Wang, Diazirines as potential molecular imaging tags: probing the requirements for efficient and long-lived SABRE-induced hyperpolarization, Angew. Chem. 129 (2017) 12280–12284.
[32] J.-B. Hövener, S. Knecht, N. Schwaderlapp, J. Hennig, D. von Elverfeldt, Continuous Re-hyperpolarization of nuclear spins using parahydrogen: theory and experiment, Chem. Phys. Chem. 15 (2014) 2451–2457.
[33] P. Rovedo, S. Knecht, T. Baumlisberger, A.L. Cremer, S.B. Duckett, R.E. Mewis, G. G. Green, M. Burns, P.J. Rayner, D. Leibfritz, J.G. Korvink, J. Hennig, G. Putz, D. von Elverfeldt, J.B. Hovener, Molecular MRI in the earth's magnetic field using continuous hyperpolarization of a biomolecule in water, J. Phys. Chem. B 120 (2016) 5670–5677.
[34] J.R. Lindale, S.L. Eriksson, C.P. Tanner, Z. Zhou, J.F. Colell, G. Zhang, J. Bae, E.Y. Chekmenev, T. Theis, W.S. Warren, Unveiling coherently driven hyperpolarization dynamics in signal amplification by reversible exchange, Nat. Commun. 10 (2019) 395.
[35] A.N. Pravdivtsev, A.V. Yurkovskaya, N.N. Lukzen, H.-M. Vieth, K.L. Ivanov, Exploiting level anti-crossings (LACs) in the rotating frame for transferring spin hyperpolarization, Phys. Chem. Chem. Phys. (2014).
[36] A.N. Pravdivtsev, I.V. Skovpin, A.I. Svyatova, N.V. Chukanov, L.M. Kovtunova, V. I. Bukhtiyarov, E.Y. Chekmenev, K.V. Kovtunov, I.V. Koptyug, J.-B. Hövener, Chemical exchange reaction effect on polarization transfer efficiency in SLIC-SABRE, J. Phys. Chem. A 122 (2018) 9107–9114.
[37] T. Theis, N.M. Ariyasingha, R.V. Shchepin, J.R. Lindale, W.S. Warren, E.Y. Chekmenev, Quasi-resonance signal amplification by reversible exchange, J. Phys. Chem. Lett. 9 (2018) 6136–6142.
[38] S. Knecht, A.S. Kiryutin, A.V. Yurkovskaya, K.L. Ivanov, Re-polarization of nuclear spins using selective SABRE-INEPT, J. Magn. Reson. 287 (2018) 10–14.
[39] S.S. Roy, G. Stevanato, P.J. Rayner, S.B. Duckett, Direct enhancement of nitrogen-15 targets at high-field by fast ADAPT-SABRE, J. Magn. Reson. 285 (2017) 55–60.
[40] J.F.P. Colell, A.W.J. Logan, Z. Zhou, J.R. Lindale, R. Laasner, R.V. Shchepin, E.Y. Chekmenev, V. Blum, W.S. Warren, S.J. Malcolmson, T. Theis, Rational ligand choice extends the SABRE substrate scope, Chem. Comm. (Under review).
[41] C.R. Bowers, D.P. Weitekamp, Parahydrogen and synthesis allow dramatically enhanced nuclear alignment, J. Am. Chem. Soc. 109 (1987) 5541–5542.
[42] S.J. DeVience, R.L. Walsworth, M.S. Rosen, Dependence of nuclear spin singlet lifetimes on RF spin-locking power, J. Magn. Reson. 218 (2012) 5–10.
[43] G. Pileio, M.H. Levitt, Theory of long-lived nuclear spin states in solution nuclear magnetic resonance. II. Singlet spin locking, J. Chem. Phys. 130 (2009).
[44] A.N. Pravdivtsev, A.V. Yurkovskaya, H. Zimmermann, H.-M. Vieth, K.L. Ivanov, Transfer of SABRE-derived hyperpolarization to spin-1/2 heteronuclei, RSC Adv. 5 (2015) 63615–63623.
[45] S. Knecht, A.S. Kiryutin, A.V. Yurkovskaya, K.L. Ivanov, Efficient conversion of anti-phase spin order of protons into 15N magnetisation using SLIC-SABRE, Mol. Phys. (2018) 1–10.
[46] T. Theis, Y. Feng, T. Wu, W.S. Warren, Composite and shaped pulses for efficient and robust pumping of disconnected eigenstates in magnetic resonance, J. Chem. Phys. 140 (2014).